HCV-related liver disease. Recently, several studies were published about estimation of hepatitis stages, using one or more serum biomarkers. Discriminant functions or multivariate analyses demonstrated that approximately 60–90% of patients with chronic hepatitis C were correctly classified as mild hepatitis and severe hepatitis with advanced fibrosis.[5–16] The usefulness of the discriminant functions was, however, less valuable up to the present time for a few reasons. First, these functions were made for the purpose of discrimination of severe hepatic fibrosis from mild fibrosis, and four histological classifications (F1, F2, F3 and F4) were selected in almost of the studies. Second, some studies analyzed both hepatitis B virus and HCV infection, although the significance and actual values of each liver function test in the evaluation of the severity of liver disease were not similar among each viral hepatitis and alcoholic liver disease. Third, biochemical markers for liver fibrosis (e.g. hyaluronic acid, type IV collagen, procollagen III peptide)[17–19] were not always included in those previous studies.

We tried to generate a function estimating fibrotic stages of HCV-related chronic hepatitis, which were objectively diagnosed by liver biopsy. The purpose of this study is, therefore, to make a reliable multiple regression function and to obtain practical coefficients for significant variables also using fibrotic markers.

METHODS

Patients

A TOTAL OF 605 Japanese patients with chronic hepatitis C were recruited for the study from eight hospitals in Japan: Toranomon Hospital, Hiroshima University Hospital (K. Chayama, M.D.), Ehime University Hospital (M. Onji, M.D.), Musashino Red Cross Hospital (N. Izumi, M.D.), Shishu University Hospital (E. Tanaka, M.D.), Showa University Hospital (M. Imawari, M.D.), Osaka University Hospital (T. Takehara, M.D.) and Kagoshima University Hospital (H. Tsubouchi, M.D.). Inclusion criteria for this study were: (i) positive HCV antibody for more than 6 months; (ii) persistent or intermittent elevation in aspartate aminotransferase (AST)/alanine aminotransferase (ALT) levels; and (iii) liver biopsy showing chronic hepatitis (F1, F2, F3 or F4). We excluded those patients with overt alcoholic liver disease or fatty liver, association of other types of liver disease (e.g. hepatitis B, primary biliary cirrhosis, autoimmune hepatitis), or those associated with hepatocellular carcinoma or other malignancy. Among the patients, 603 fulfilled the conditions for the study: complete demographic data, basic laboratory data of hematology and biochemistry, required liver biopsy specimens, and sufficient amount of frozen sera. We also excluded an additional 22 patients with eventual histological diagnosis of F0 stage.

Finally, a total of 581 patients who were diagnosed as having chronic hepatitis or cirrhosis (F1, F2, F3 or F4) were analyzed for the following hematological, biochemical and histopathological examination. There were 305 males and 276 females aged 15–78 with a median of 55 years.

All the patients presented written informed consent in individual hospitals and medical centers, and the study was approved by each ethical committee.

Hematological and biochemical examination

Hematological and standard biochemical evaluation had been performed in each medical institution: white blood cell, red blood cell count, hemoglobin, platelet count, total bilirubin, AST, ALT, AST/ALT ratio (AAR), γ-glutamyltransferase (GGT), total protein, albumin and γ-globulin.

Special biochemical examinations including fibrotic markers were carried out using stored frozen sera at −20°C or lower: α2-macroglobulin, haptoglobin concentration, haptoglobin typing, apolipoprotein A1, hyaluronic acid, tissue inhibitor of matrix metalloproteinase (TIMP)-1, TIMP-2, procollagen III peptide and type IV collagen 7S.

Histological diagnosis of chronic hepatitis and cirrhosis

All of the 581 cases fulfilled required standards of histological evaluation: sufficient length of specimen, hematoxylin–eosin staining and at least one specimen with fiber staining. Four independent pathologists (Y. T., J. F., F. K. and T. F.), who were not informed of patients' background and laboratory features except for age and sex, evaluated the 581 specimens regarding the stages of fibrosis and activity. Pathological classification of chronic hepatitis staging was based on Desmet *et al.*[20]

Before judgment of histological staging of individual specimens, the pathologists discussed objective and reproducible judgment of pathological diagnosis of hepatitis. They made a panel for obvious criteria using typical microscopic pictures for each stage, and it was always referred to during the procedure of pathological judgment. When inconsistent results were found in the diagnosis of stage of hepatitis among the pathologists, the final judgment was accepted as the majority rule among them.

Statistical analysis

Non-parametric procedures were employed for the analysis of background characteristics and laboratory data among patients in each stage, including Mann–Whitney *U*-test, Kruskal–Wallis test and χ^2-test.

The normality of the distribution of the data was evaluated by Kolmogorov–Smirnov one-sample test. Because certain variables partly did not conform to a normal distribution, natural logarithmic transformation of bilirubin, AST, ALT, GGT, α2-macroglobulin, hyaluronic acid, type IV collagen 7S and TIMP-2 were also analyzed in the following calculation. The natural logarithmic transformation of the results yielded a normal distribution or symmetrical distribution for all the analyzed factors. After the procedures, the following multiple regression analysis became rationally robust against deviations from normal distribution. In order to avoid introducing into the model any variables that were mutually correlated, we checked the interaction between all pairs of the variables by calculating variance of inflation factors. Of the highly correlated variables, less significant factors were removed from the viewpoint of multicollinearity.

Multivariate regression analysis was performed using 305 patient data from Toranomon Hospital (training dataset), to generate training data of predicting function. We used a stepwise method for selection of informative subsets of explanatory variables in the model. Multiple regression coefficient and coefficient of determination are also taken into account in the selection of variables. Next, we validated the obtained predictive function using the remaining 276 patient data from the other seven liver institutions (validation dataset).

A *P*-value of less than 0.05 with two-tailed test was considered to be significant. Data analysis was performed using the computer program SPSS version 19.[21]

For evaluation of the efficiency and usefulness of obtained function for estimation of fibrosis, we compared various fibrotic scores for hepatitis C, including AAR,[8] AST-to-platelet ratio index (APRI),[12] FIB-4[13] and FibroTest.[9]

RESULTS

Pathological diagnosis

FOUR PATHOLOGISTS INDEPENDENTLY judged the fibrotic stages and inflammatory activity for 581 specimens of chronic hepatitis/cirrhosis caused by HCV. A total of 328 patients (56.5%) had a fibrotic stage of F1, 153 (26.3%) F2, 73 (12.6%) F3 and 27 (4.6%) F4. In the training subgroup ($n = 305$), judgment of F1 was made in 172, F2 in 80, F3 in 37 and F4 in 16. In the validation group ($n = 276$), judgment as F1 was made in 156, F2 in 73, F3 in 36 and F4 in 11.

According to hepatitis activity classification, A0 was found in nine patients (1.52%), A1 in 350 (60.2%), A2 in 198 (34.1%) and A3 in 24 (4.1%).

Laboratory data of each hepatitis stage in training group

There were 161 males and 144 females with a median age of 54 years (range, 22–69). Laboratory data of the 305 patients in the training group are shown in Table 1. Although several individual items were well correlated with the severity of hepatic fibrosis, significant overlap values were noted among F1 to F4 stages: platelet count, GGT, γ-globulin, hyaluronic acid and type IV collagen 7S.

Regression function generated from training patient group

After stepwise variable selection, multivariate regression analysis finally obtained the following function: $z = 2.89 \times ln$ (type IV collagen 7S) (ng/mL) $- 0.011 \times$ (platelet count) ($\times 10^3$/mm^3) $+ 0.79 \times ln$ (total bilirubin) (ng/mL) $+ 0.39 \times ln$ (hyaluronic acid) (μm/L) $-$ 1.87. Median values of the fibrotic score of F1 ($n = 172$), F2 ($n = 80$), F3 ($n = 37$) and F4 stages ($n = 16$) were calculated as 1.00, 1.45, 2.82 and 3.83, respectively (Fig. 1). The multiple regression coefficient and coefficient of determination were 0.56 and 0.32, respectively.

A 55-year-old man with F1 fibrotic stage (Fig. 2a) showed serum type IV collagen concentration as 3.8 ng/mL, platelet as 152×10^3 count/mm^3, total bilirubin as 0.8 mg/dL and hyaluronic acid as 16 μg/L. The regression function provided his fibrotic score as 1.16. Another man aged 43 years had F3 fibrosis with severe hepatitis activity of A3 on histological examination (Fig. 2b). His type IV collagen was 11.0 ng/mL, platelet 162×10^3 count/mm^3, total bilirubin 0.7 mg/dL and hyaluronic acid 189 μg/L, and regression function calculated his fibrotic score as 4.98.

Validation of discriminant function

Validation data of 276 patients (Table 2) were collected from the other seven institutions in Japan. When applying the regression function for the validation set, the fibrotic score for hepatitis C (FSC) demonstrated good reproducibility, showing 1.10 in patients with chronic hepatitis of F1 ($n = 156$), 2.35 in F2 ($n = 73$), 3.16 in F3 ($n = 36$) and 3.58 in F4 ($n = 11$) (Fig. 3). Although F4

Table 1 Demography and laboratory data of 305 patients in training group

	F1 ($n = 172$)	F2 ($n = 80$)	F3 ($n = 37$)	F4 ($n = 16$)
Demography				
Males : females	97:75	38:42	20:17	6:10
Age (median, range)	51 (22–69)	55 (29–68)	55 (27–69)	56.5 (29–65)
Laboratory data (median, range)				
WBC ($\times 10^3/mm^3$)	4.7 (2.0–10.1)	4.3 (2.3–8.5)	4.5 (2.9–6.8)	4.7 (3.3–6.9)
Hemoglobin(g/dL)	14.6 (11.0–18.2)	14.4 (9.3–17.4)	14.6 (11.5–17.7)	14.55 (12.1–16.5)
Platelet ($\times 10^3/mm^3$)	183 (52–364)	161 (82–387)	131 (74–237)	124 (7.7–191)
Albumin (g/dL)	4.1 (2.3–4.9)	4.0 (3.5–4.6)	3.9 (3.1–4.6)	3.8 (3.3–4.3)
Bilirubin (mg/dL)	0.8 (0.2–1.9)	0.7 (0.3–1.7)	0.9 (0.4–7.5)	0.8 (0.5–7.4)
AST (IU/L)	42 (16–386)	61 (16–332)	63 (13–238)	71 (30–160)
ALT (IU/L)	60.5 (12–1664)	84.5 (10–647)	108 (27–415)	90.5 (36–264)
γ-GTP (IU/L)	40 (7–383)	48 (10–262)	54 (13–209)	58 (21–195)
γ-Globulin (g/dL)	1.47 (0.58–3.40)	1.61 (1.02–2.41)	1.69 (0.66–2.64)	1.79 (1.22–2.73)
γ-Globulin (%)	19.4 (10.0–40.5)	20.9 (14.0–28.3)	21.3 (8.1–30.4)	22.7 (16.5–36.9)
α2-Macroglobulin (mg/dL)	269 (123–505)	335 (154–551)	369 (183–627)	317 (207–511)
Haptoglobin (mg/dL)	94.5 (<5–265)	75.5 (<5–263)	56 (<5–2031)	75 (30–142)
Apolipoprotein A1 (mg/dL)	132 (71–209)	131 (73–207)	124 (98–166)	121 (83–153)
Hyaluronic acid (μg/L)	25 (<5–407)	41.5 (<5–263)	71 (<5–326)	89.5 (5–246)
TIMP-1 (ng/mL)	165 (73–291)	173 (97–302)	182 (126–308)	192.5 (128–260)
TIMP-2 (ng/mL)	77.5 (31–210)	80 (34–307)	76 (46–143)	78 (58–110)
Procollagen III peptide (U/mL)	0.75 (0.47–1.50)	0.805 (0.61–1.70)	0.86 (0.53–1.50)	1.05 (0.66–1.60)
Type IV collagen 7S (ng/mL)	4.0 (1.7–73)	4.3 (2.1–11.0)	5.2 (3.2–11.0)	5.8 (4.3–9.4)

γ-GTP, γ-glutamyl transpeptidase; ALT, alanine aminotransferase; AST, aspartate aminotransferase; TIMP, tissue inhibitor of matrix metalloproteinase; WBC, white blood cell.

fibrotic stage consisted of only 11 patients and the score 3.58 was regarded as a rather low value, the scores of other stages of fibrosis were concordant with histological fibrosis.

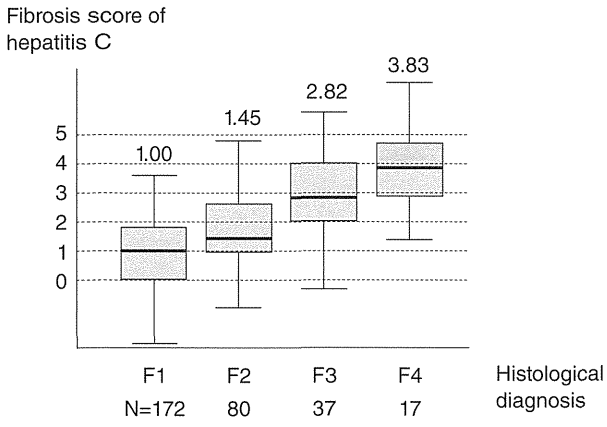

Figure 1 Box and whisker plots of fibrotic score of each group of histological fibrosis in the training dataset. Fibrotic score of hepatitis C (FSC) was generated by the function, $z = 2.89 \times ln$ (type IV collagen 7S) (ng/mL) $- 0.011 \times$ (platelet count) ($\times 10^3/mm^3$) $+ 0.79 \times ln$ (total bilirubin) (mg/dL) $+ 0.39 \times ln$ (hyaluronic acid) (μg/L) $- 1.87$.

Comparisons of efficacy with various fibrotic scores (Fig. 4)

In order to evaluate the efficacy and usefulness of the obtained FSC, we compared with previously reported fibrotic scores using training data. AAR, APRI, FIB-4 and FibroTest showed only slight correlation with actual histological stage. APRI and FIB-4 demonstrated increasing trends of the score associated with histological fibrosis, but significant overlapping scores were found through F1 to F4. Spearman's correlation coefficients of AAR, APRI, FIB-4 and FibroTest were 0.021 ($P = 0.707$), 0.462 ($P < 0.001$), 0.440 ($P < 0.001$) and 0.415 ($P < 0.001$), respectively. Our FSC showed Spearman's correlation coefficient of 0.572 ($P < 0.001$), and was of much higher value than the others.

DISCUSSION

RECOGNITION OF SEVERITY of chronic hepatitis is essential in managing patients with chronic HCV infection: estimation of length of infection, existence of any previous hepatitis activity, presumption of current fibrotic stage, and prediction of future fibrotic progression and hepatocarcinogenesis. Differential diagnosis of cirrhosis from chronic hepatitis is especially important

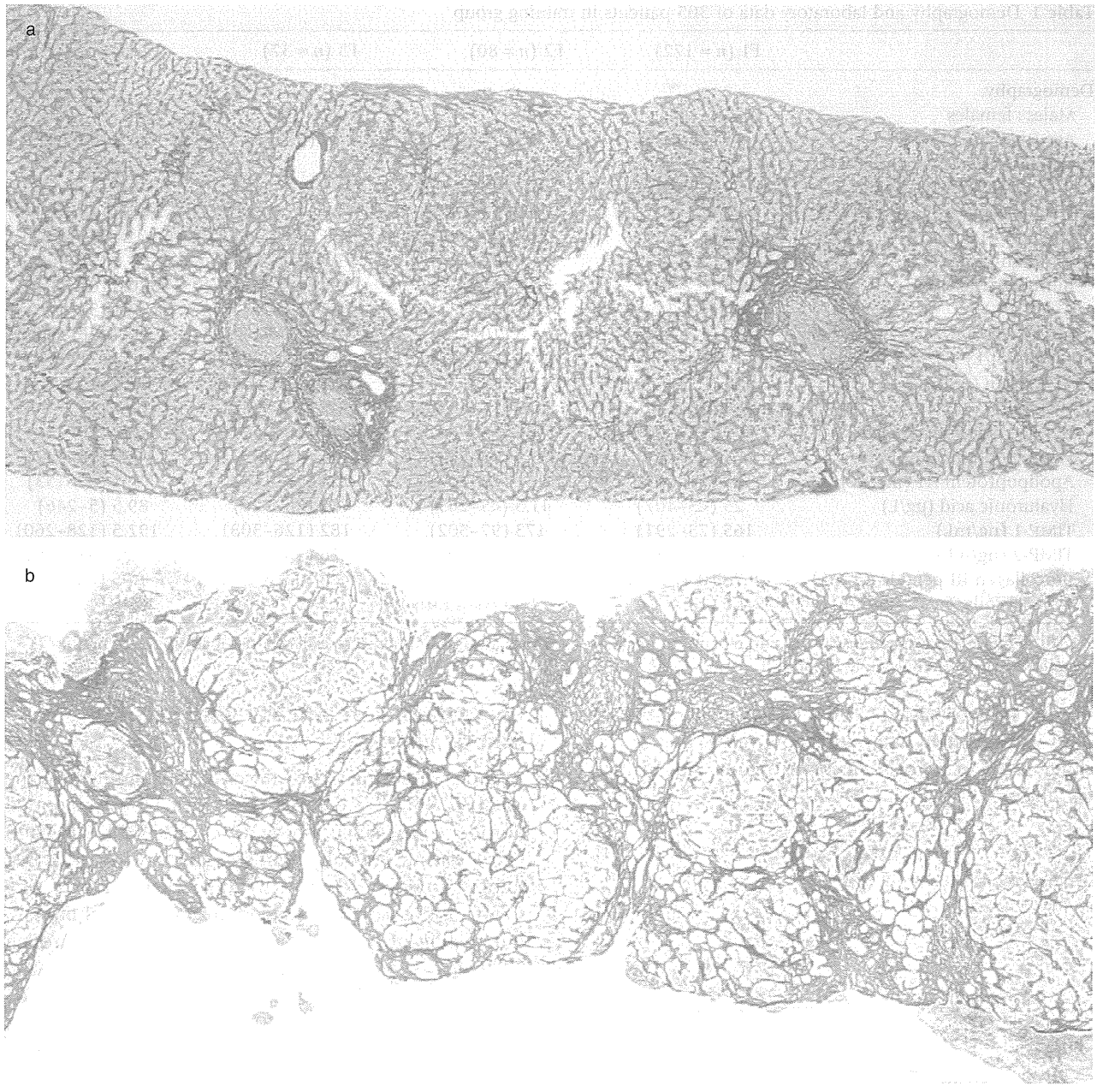

Figure 2 Case presentations of the training set. (a) A 55-year-old man with F1 fibrosis. Final regression function provided his fibrotic score as 1.16. (b) A 43-year-old man with F3 fibrosis with severe hepatitis activity. His regression coefficient was calculated as 4.98 (silver stain, ×40).

in the evaluation of chronic HCV infection. Identification of liver cirrhosis often leads to an important change in management of the patients: needs for fiberscopic examination for esophageal varices, ultrasonographic exploration for the association of liver cancer, and prediction of hepatic decompensation.

Recently, non-invasive estimation of severity of liver fibrosis has been reported in patients with HCV-related chronic hepatitis.[6–14] However, these studies were principally aimed at differentiation of advanced fibrotic stages of F3 or F4 from mild fibrotic stages of F1 or F2. Those discriminative functions were insufficient to

Table 2 Demography and laboratory data of 276 patients in validation group

	F1 ($n = 156$)	F2 ($n = 73$)	F3 ($n = 36$)	F4 ($n = 11$)
Demography				
Males : females	83:73	42:31	13:23	6:5
Age (median, range)	55 (15–74)	58 (32–77)	62.5 (30–78)	51 (38–73)
Laboratory data (median, range)				
WBC ($\times 10^3/mm^3$)	5.1 (2.1–10.5)	4.8 (2.6–9.0)	4.85 (2.3–14.2)	3.9 (3.2–6.0)
Hemoglobin (g/dL)	14.2 (8.9–17.7)	14.4 (11.8–17.4)	14.1 (10.1–16.4)	13.6 (8.9–16.3)
Platelet ($\times 10^3/mm^3$)	183 (59–440)	153 (80–265)	136 (64–348)	135 (79–153)
Albumin (g/dL)	4.3 (3.1–5.3)	4.3 (3.3–5.2)	4.05 (3.0–5.5)	3.9 (3.0–4.7)
Bilirubin (mg/dL)	0.7 (0.2–8.7)	0.7 (0.2–1.7)	0.8 (0.2–2.5)	0.8 (0.4–11.0)
AST (IU/L)	35 (11–1390)	49 (19–183)	80 (20–190)	96 (29–257)
ALT (IU/L)	49 (11–1635)	62 (12–575)	84 (14–218)	115 (29–303)
γ-GTP (IU/L)	35 (11–600)	52 (10–497)	51 (14–236)	112 (17–312)
γ-Globulin (g/dL)	1.47 (0.70–2.14)	1.60 (0.80–2.37)	1.71 (0.63–2.62)	2.19 (1.70–2.82)
γ-Globulin (%)	19.5 (9.2–26.4)	20.8 (10.8–30.8)	22.4 (9.5–29.9)	27.4 (21.8–35.3)
α2-Macroglobulin (mg/dL)	271.5 (126–572)	381 (172–573)	405.5 (196–594)	468 (242–655)
Haptoglobin (mg/dL)	95 (<5–305)	80 (<5–223)	63.5 (<5–192)	65 (<5–130)
Apolipoprotein A1 (mg/dL)	126 (45–198)	127 (63–191)	116 (46–172)	108 (62–171)
Hyaluronic acid (μg/L)	37.5 (<5–1260)	68 (5–1000)	140.5 (23–2610)	159 (33–364)
TIMP-1 (ng/mL)	157.5 (77–301)	172 (89–355)	188.5 (99–430)	192 (112–320)
TIMP-2 (ng/mL)	70 (21–294)	73 (21–207)	89 (27–280)	76 (36–120)
Procollagen III peptide (U/mL)	0.73 (0.52–8.30)	0.81 (0.53–1.60)	1.00 (0.63–1.90)	1.00 (0.68–1.60)
Type IV collagen 7S (ng/mL)	3.9 (1.2–12.0)	4.5 (2.3–9.9)	5.8 (2.8–16.0)	6.1 (4.6–10.0)

γ-GTP, γ-glutamyl transpeptidase; ALT, alanine aminotransferase; AST, aspartate aminotransferase; TIMP, tissue inhibitor of matrix metalloproteinase; WBC, white blood cell.

recognize the stepwise progression of viral hepatitis from F1 through F4. This dichotomy (mild or severe) of chronic hepatitis C seemed less valuable in the study of disease progression, disease control abilities of antiviral drugs and estimation of histological improvement after anti-inflammatory drugs. A histology-oriented, practical and reliable formula is therefore required for the diagnosis and investigation of chronic hepatitis C.

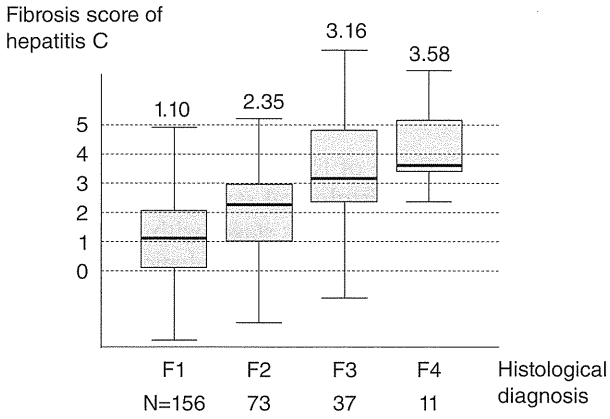

Figure 3 Box and whisker plots of fibrotic score of each group of histological fibrosis in the validation dataset. Fibrotic score of hepatitis C (FSC) was generated by the function, $z = 2.89 \times ln$ (type IV collagen 7S) (ng/mL) $- 0.011 \times$ (platelet count) ($\times 10^3/mm^3$) $+ 0.79 \times ln$ (total bilirubin) (ng/mL) $+ 0.39 \times ln$ (hyaluronic acid) (μg/L) $- 1.87$.

This study was aimed to establish non-invasive evaluation and calculation of liver fibrosis for patients with chronic HCV infection. Although it was retrospectively performed as a multicenter study of eight institutions, judgment of histological diagnosis was independently performed by four pathologists in the other hospital, informed of nothing except for the patient's age, sex and positive HCV infection. Objective judgment of the histological staging and grading in sufficient biopsy specimens could be obtained.

As many as 581 patients with chronic hepatitis C were analyzed in this study, who had been diagnosed as having chronic hepatitis or cirrhosis by liver biopsy performed in experienced liver units in Japan. To obtain the most suitable equation approximating histological fibrotic stage, multivariate analysis was performed using two demographic parameters (age and sex) and 21 hematological and biochemical markers with or without logarithmic transformation. They included many kinds of fibrotic markers: α2-macroglobulin, haptoglobin concentration, haptoglobin typing, apolipo-

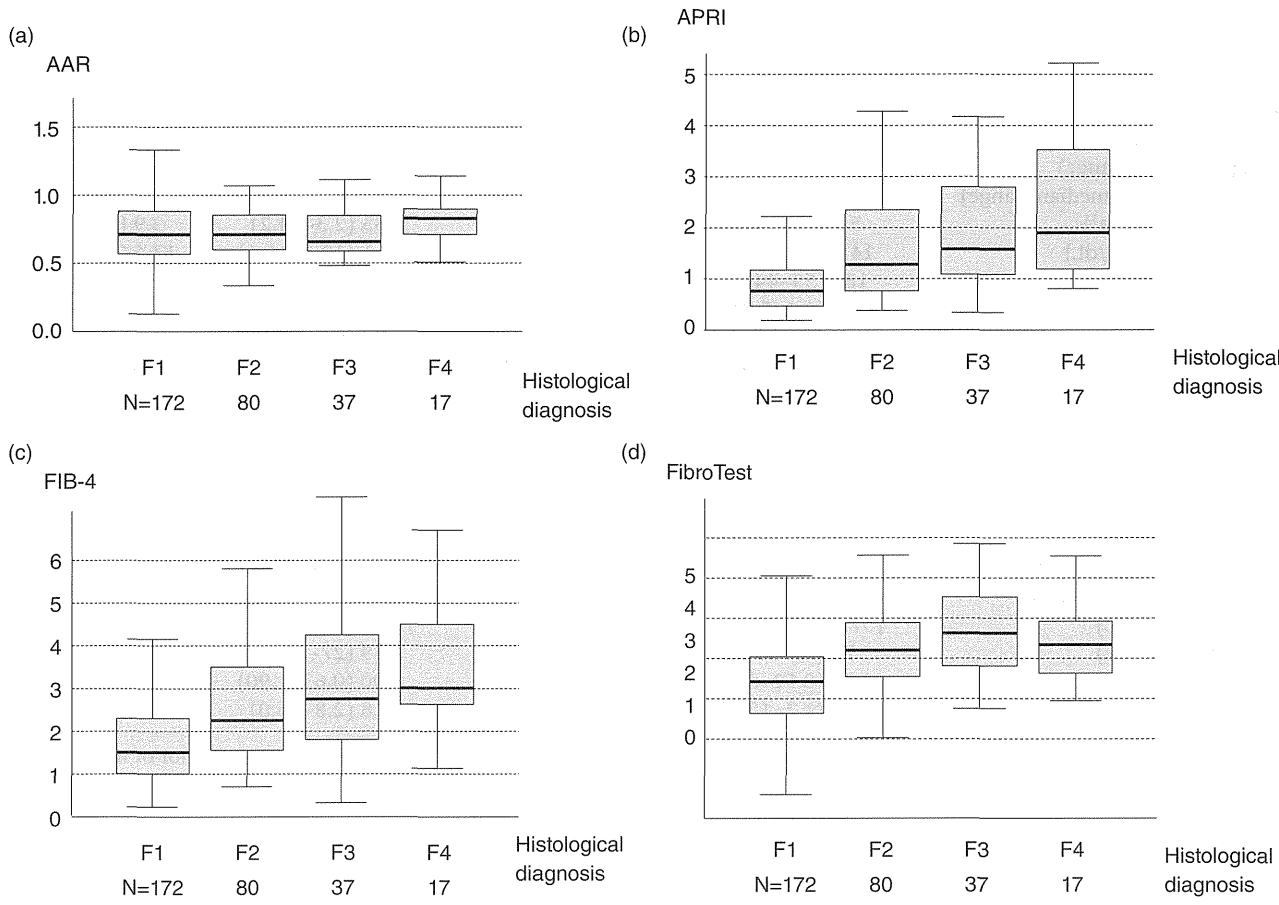

Figure 4 Previously published fibrotic scores: (a) aspartate aminotransferase (AST)/alanine aminotransferase (ALT) ratio (AAR),[8] (b) AST-to-platelet ratio index (APRI), calculated by AST / (upper limit of normal of AST) / (platelet count [$\times 10^9$/L]) $\times$ 100.[12] (c) FIB-4 score, calculated by age $\times$ AST [IU/L] / (platelet count [$\times 10^9$/L] $\times$ ALT [IU/L]$^{0.5}$).[13] (d) FibroTest score regression coefficient was: Z = 4.467 $\times \log^{10}$ (α2-macroglobulin [g/L]) − 1.357 $\times \log^{10}$ (haptoglobin [g/L]) + 1.017 $\times \log^{10}$ [γ-glutamyltransferase [GGT] [IU/L]) + 0.0281 $\times$ (age [years]) + 1.737 $\times \log^{10}$ (bilirubin [μm/L]) − 1.184 $\times \log^{10}$ (apolipoprotein A1 [g/L]) + 0.301 $\times$ (sex [female = 0, male = 1]) − 5.54.[9]

protein A1, hyaluronic acid, TIMP-1, TIMP-2, procollagen III peptide and type IV collagen 7S. Multiple regression analysis finally generated a first-degree polynomial function consisting of four variables: type IV collagen 7S, platelet count, bilirubin and hyaluronic acid. A constant numeral (−1.87) was finally adjusted in the regression equation in order to obtain fitted figures for fibrotic stages of F1, F2, F3 and F4. From the magnitude of the standardized partial regression coefficient of individual variable in the function, *ln* (type IV collagen 7S) demonstrated the most potent contribution toward the prediction of liver fibrosis. Platelet count and *ln* (bilirubin) proved to be the second and third distinctive power in the model, respectively.

The obtained figure of FSC was generated to imitate actual "F factor" of histological staging. FSC was sufficiently fitted to actual fibrotic stages with certain overlapping as was usually found in histological ambiguity judged by pathologists. Because judgment of fibrosis in chronic hepatitis often shows a transitional histological staging, pathological examination could not always achieve a clear-cut diagnosis discriminating F1, F2, F3 or F4. Considering the limitation of pathological difficulty in differentiation of the four continuous disease entities, the obtained regression function showed satisfactory high accuracy rates in the prediction of liver disease severity. FSC can provide one or two decimal places (e.g. 2.4 or 2.46) and the utility of the score is possibly higher

than mere histological staging of F1, F2, F3 or F4. The reproducibility was confirmed by the remaining 276 patients' data obtained from the other seven hospitals. Although the validation data were collected from different geographic area and different chronologic situation, FSC showed similar results in prediction of histological staging.

Fibrotic score for hepatitis C seemed a very useful quantitative marker in evaluating severity of fibrotic severity of hepatitis C patients without invasive procedures and without any specialized ultrasonography or magnetic resonance imaging. FSC also has an advantage of measurement, in which old blood samples are available for retrospective assessment of varied clinical settings: old sera from 20 years ago at the time of initial liver biopsy, or paired sera before and after a long-term anti-inflammatory therapy, for example. These kinds of retrospective assessments of fibrotic staging will be valuable in estimating a long-term progression of liver disease, in evaluating efficacy of a long-term medication or other medical intervention, or in making a political judgment from the viewpoint of socioeconomic efficacy.

The score can be calculated for any patients with chronic HCV infection. Although this multiple regression model dealt with appropriate logarithmic transformation for non-normal distribution parameters, the regression analysis was based on a linear regression model. Very slight fibrosis can be calculated as less than 1.00, which is commonly found with a slight degree of chronic hepatitis with a tiny fibrotic change as F0. Very severe fibrosis may be calculated as more than 4.00, which is an imaginable and nonsense number in the scoring system of fibrosis. FSC is, however, very useful and valuable in real clinical setting. Estimation of severity of liver fibrosis in outpatient clinics, evaluation of natural progression of patients' fibrosis over 10 years, and assessment of a long-term administration of interferon in patients with chronic hepatitis C from the viewpoint of fibrotic change. In this study, because certain patients actually had a history of interferon administration, regression of liver fibrosis during and after the treatment could be assessed when prior sera were available for serial evaluation of FSC. We can also expect the usefulness of evaluation of carcinogenic risk after sustained virological response, and stage progression with alcohol intake or obesity-induced steatosis. Recent development of new directly acting antiviral agents require evaluation for long-term histological advantage, for aggravation of hepatitis stage during viral and biochemical breakthrough caused by HCV mutation, estimation of future carcinogenic risk, and even for the best way of management of patients with chronic hepatitis C. FSC seems one of the ideal methods of approximation for fibrotic stage of chronic hepatitis C. Repeated measurement is quite suitable for patients with an unestablished treatment or trial, every 1 or 2 years, for example. Because the current regression function was generated from the data of HCV-related chronic liver disease, this equation would not be suitable for the recognition of HBV-related chronic liver disease,[22] alcoholic liver disease and other congenital or autoimmune liver diseases. To recognize the latter diseases, other studies about individual diseases must be performed.

We compared the usefulness of the FSC with that of other fibrotic scores.[8,9,12,13] More simple and inexpensive AAR or APRI could not well estimate fibrotic stages with poor correlation coefficients of 0.021 and 0.462, which were much lower than the coefficient of FSC of 0.572. FibroTest, which contained three costly fibrotic markers (α2-macroglobulin, haptoglobin and apolipoprotein A1), also showed a low correlation coefficient of 0.415, suggesting that the usefulness was limited in HCV positive Asian patients. Although FIB-4 demonstrated the best coefficient of 0.440 among the fibrotic scores, significant overlaps were found between neighboring stages and obtained scores were not coordinated for rea17l histological classification. Because this study also measured those special markers included in FibroTest, the ability of discrimination of fibrotic stages could be compared among the five fibrotic scoring systems.

In conclusion, FSC was a useful and reliable biomarker for prediction of liver fibrosis in patients with chronic HCV infection. FSC is expected to be introduced and utilized in varied kinds of studies and trials. Its accuracy and reproducibility require further validation using more numbers of patients in several countries other than Japan.

ACKNOWLEDGMENTS

THIS STUDY WAS proposed and initiated by Dr Shiro Iino, and the project was performed by a grant from the Viral Hepatitis Research Foundation of Japan.

REFERENCES

1 Sandrin L, Fourquet B, Hasquenoph JM *et al.* Transient elastography: a new noninvasive method for assessment of hepatic fibrosis. *Ultrasound Med Biol* 2003; **29**: 1705–13.
2 Hanna RF, Kased N, Kwan SW *et al.* Double-contrast MRI for accurate staging of hepatocellular carcinoma in patients with cirrhosis. *AJR Am J Roentgenol* 2008; **190**: 47–57.

3 Hagiwara M, Rusinek H, Lee VS *et al.* Advanced liver fibrosis: diagnosis with 3D whole-liver perfusion MR imaging – initial experience. *Radiology* 2008; **246:** 926–34.
4 Taouli B, Chouli M, Martin AJ, Qayyum A, Coakley FV, Vilgrain V. Chronic hepatitis: role of diffusion-weighted imaging and diffusion tensor imaging for the diagnosis of liver fibrosis and inflammation. *J Magn Reson Imaging* 2008; **28:** 89–95.
5 Williams AL, Hoofnagle JH. Ratio of serum aspartate to alanine aminotransferase in chronic hepatitis. Relationship to cirrhosis. *Gastroenterology* 1988; **95:** 734–9.
6 Poynard T, Bedossa P. Age and platelet count: a simple index for predicting the presence of histological lesions in patients with antibodies to hepatitis C virus. METAVIR and CLINIVIR Cooperative Study Groups. *J Viral Hepat* 1997; **4:** 199–208.
7 Sheth SG, Flamm SL, Gordon FD, Chopra S. AST/ALT ratio predicts cirrhosis in patients with chronic hepatitis C virus infection. *Am J Gastroenterol* 1998; **93:** 44–8.
8 Giannini E, Botta F, Fasoli A *et al.* Progressive liver functional impairment is associated with an increase in AST/ALT ratio. *Dig Dis Sci* 1999; **44:** 1249–53.
9 Imbert-Bismut F, Ratziu V, Pieroni L, Charlotte F, Benhamou Y, Poynard T, MULTIVIRC Group. Biochemical imarkers of liver fibrosis in patients with hepatitis C virus infection: a prospective study. *Lancet* 2001; **357:** 1069–75.
10 Wai CT, Greenson JK, Fontana RJ *et al.* A simple noninvasive index can predict both significant fibrosis and cirrhosis in patients with chronic hepatitis C. *Hepatology* 2003; **38:** 518–26.
11 Benlloch S, Berenguer M, Prieto M, Rayón JM, Aguilera V, Berenguer J. Prediction of fibrosis in HCV-infected liver transplant recipients with a simple noninvasive index. *Liver Transpl* 2005; **11:** 456–62.
12 Chrysanthos NV, Papatheodoridis GV, Savvas S *et al.* Aspartate aminotransferase to platelet ratio index for fibrosis evaluation in chronic viral hepatitis. *Eur J Gastroenterol Hepatol* 2006; **18:** 389–96.
13 Sterling RK, Lissen E, Clumeck N *et al.* Develoment of a simple noninvasive index to predict significant fibrosis in patients with HIV/HCV coinfection. *Hepatology* 2006; **43:** 1317–25.
14 Alsatie M, Kwo PY, Gingerich JR *et al.* A multivariable model of clinical variables predicts advanced fibrosis in chronic hepatitis C. *J Clin Gastroenterol* 2007; **41:** 416–21.
15 Attallah AM, Abdallah SO, El Sayed AS *et al.* Non-invasive predictive score of fibrosis stages in chronic hepatitis C patients based on epithelial membrane antigen in the blood in combination with routine laboratory markers. *Hepatol Res* 2011; **41:** 1075–84.
16 Kalantari H, Hoseini H, Babak A, Yaran M. Validation of hepascore as a predictor of liver fibrosis in patients with chronic hepatitis C infection. *Hepat Res Treat* 2011; **2011:** 972759.
17 Engstrom-Laurent A, Loof L, Nyberg A, Schroder T. Increased serum levels of hyaluronate in liver disease. *Hepatology* 1985; **5:** 638–42.
18 Murawaki Y, Ikuta Y, Koda M, Kawasaki H. Serum type III procollagen peptide, type IV collagen 7S domain, central triple-helix of type IV collagen and tissue inhibitor of metalloproteinases in patients with chronic viral liver disease: relationship to liver histology. *Hepatology* 1994; **20:** 780–7.
19 Fabris C, Falleti E, Federico E, Toniutto P, Pirisi M. A comparison of four serum markers of fibrosis in the diagnosis of cirrhosis. *Ann Clin Biochem* 1997; **34:** 151–5.
20 Desmet VJ, Gerber M, Hoofnagle JH, Manns M, Sheuer PJ. Classification of chronic hepatitis: diagnosis, grading, and staging. *Hepatology* 1994; **19:** 1513–20.
21 IBM SPSS Inc. IBM SPSS for Windows. Version 19.0 manual. SPSS Japan Inc., an IBM company. Armonk NY, USA, 2009.
22 Ikeda K, Izumi N, Tanaka E *et al.* Fibrosis score consisting of four serum markers successfully predicts pathological fibrotic stages of chronic hepatitis B. *Hepatol Res* 2012; **43:** 596–604.

Biochemical and Biophysical Research Communications 438 (2013) 230–235

Contents lists available at ScienceDirect

Biochemical and Biophysical Research Communications

journal homepage: www.elsevier.com/locate/ybbrc

Inhibition of microRNA122 decreases SREBP1 expression by modulating suppressor of cytokine signaling 3 expression

Chikako Shibata [a], Takahiro Kishikawa [a], Motoyuki Otsuka [a,b,*], Motoko Ohno [a], Takeshi Yoshikawa [a], Akemi Takata [a], Haruhiko Yoshida [a], Kazuhiko Koike [a]

[a] Department of Gastroenterology, Graduate School of Medicine, The University of Tokyo, Tokyo 113-8655, Japan
[b] Japan Science and Technology Agency, PRESTO, Kawaguchi, Saitama 332-0012, Japan

ARTICLE INFO

Article history:
Received 13 July 2013
Available online 24 July 2013

Keywords:
microRNA
Liver
SOCS3
SREBP
Expression regulation

ABSTRACT

While inhibition of microRNA122 (miR122) function *in vivo* results in reduced serum cholesterol and fatty acid levels, the molecular mechanisms underlying the link between miR122 function and lipid metabolism remains unclear. Because the expression of SREBP1, a central transcription factor involved in lipid metabolism, is known to be increased by suppressor of cytokine signaling 3 (SOCS3) expression, and because we previously found that SOCS3 expression is regulated by miR122, in this study, we examined the correlation between miR122 status and the expression levels of SOCS3 and SREBP1. SREBP1 expression decreased when SOCS3 expression was reduced by miR122 silencing *in vitro*. Conversely, SREBP1 expression in miR122-silenced cells was restored by enforced expression of SOCS3. Such correlations were observed in human liver tissues with different miR122 expression levels. These signaling links may explain one of the molecular mechanisms linking inhibition of miR122 function or decreased expression of miR122 to decreased fatty acid and cholesterol levels, in the inhibition of miR122 function, or in pathological status in chronic liver diseases.

1. Introduction

MiRNA122 (miR122) is the most abundant and tissue-specific miRNA in the liver [1], and inhibition of miR122 *in vivo* was shown to greatly reduce serum cholesterol and fatty acid levels [2–6]. Recently, miravirsen, a locked nucleic acid-modified DNA phosphorothioate antisense oligonucleotide against miR122, was introduced practically to reduce hepatitis C virus (HCV) RNA levels in patients with HCV infection [7]. Although the primary purpose of the trial was to inhibit HCV replication, lipid levels were also found to decrease [7]. Despite consistent results concerning miR-122-mediated lipid metabolism, the underlying molecular mechanisms remain unclear, and although the expression levels of genes associated with lipid metabolism were affected by miR-122 inhibition, these genes were not direct targets of miR122, as judged by sequence similarities.

Members of the family of sterol regulatory element-binding proteins (SREBPs) are critical regulators of cholesterol and lipid homeostasis. The SBEBP family belongs to the basic helix–loop–helix–leucine zipper (bHLH-zipper) family of transcription factors and comprises SREBP-1a, SREBP-1c, and SREBP-2. The SREBF-1 gene on chromosome 17p11.2 encodes SREBP-1a and SREBP-1c, which are generated as alternatively spliced variants. Increased SREBP activity causes cholesterol and fatty acid accumulation by activating the expression of more than 30 genes dedicated to the synthesis and uptake of cholesterol, fatty acids, triglycerides, and phospholipids, as well as the NADPH cofactor required for synthesis of these molecules [8], which increases lipid levels.

The promoter activities of SREBP1 are potently inhibited by activated STAT3 [9]. In addition, STAT3-mediated inhibition of SREBP1 expression was shown to be antagonized by co-expression of the SOCS3 protein [9]. Conversely, SOCS3 inhibition in the liver in obese mice subjected to antisense treatment was reported to completely normalize the increased expression of SREBP1, leading to dramatic amelioration of hyperlipidemia. These results indicate the importance of SOCS3 in regulating SREBP expression and subsequent lipid metabolism [9].

We recently reported that silencing miR122 in hepatocytes leads to decreased SOCS3 expression accompanied by hypermethylation of the SOCS3 promoter in a Dnmt1-independent manner [10]. In this study, we first assessed the correlated expression levels of SREBP1 in miR122-silenced and miR122 precursor-overexpressing cells. In addition, SREBP1 was recovered by enforced expression or inhibition of SOCS3 in miR122-modulated cells. We next confirmed the correlations among miR122, SOCS3, and SREBP

* Corresponding author. Address: Department of Gastroenterology, Graduate School of Medicine, The University of Tokyo, 5-3-1 Hongo, Bunkyo-ku, Tokyo 113-8655, Japan. Fax: +81 3 3814 0021.
E-mail address: otsukamo-tky@umin.ac.jp (M. Otsuka).

0006-291X/$ - see front matter © 2013 Elsevier Inc. All rights reserved.
http://dx.doi.org/10.1016/j.bbrc.2013.07.064

expression levels in human liver tissues in various pathological states with different miR122 expression levels [11]. Based on these analyses, we infer a molecular link between miR122 and lipid metabolism in miR122 inhibition and various liver pathological states.

2. Methods

2.1. Cells

The Huh7 and Hep3B human hepatocellular carcinoma cell lines were obtained from the Japanese Collection of Research Bioresources (JCRB, Osaka, Japan). Cells were maintained in Dulbecco's modified Eagle's medium (DMEM) supplemented with 10% fetal bovine serum.

2.2. Plasmids, viral production, and transduction

A miR122 precursor-expressing plasmid with a puromycin resistance gene (pCDH-miR122 with puro) and an H1 promoter-driven antisense miR122 stem–loop–stem RNA-expressing plasmid (pmiRZIP122 with puro) were constructed as described previously [10]. For double stable Hep3B cells with miR122 precursor and SOCS3 shRNA expression, a miR122 precursor with hygromycin resistance gene (pCDH-miR122 with hygro) was constructed by replacement of the puromycin resistance gene with a hygromycin resistant gene using the infusion method (Clontech, Mountain View, CA). SOCS3 shRNA-expressing lentiviral particles were purchased from Santa Cruz Biotechnology (Dallas, TX). An HA-SOCS3-expressing lentiviral construct with a neomycin resistance gene was constructed as described previously [10]. A pCDH control vector (System Biosciences, Mountain View, CA) was used as a negative control. Lentiviral particles, produced using pPACKH1 lentivector packaging plasmid mix (System Biosciences) according to the manufacturer's recommendations, were used as a negative control. Cells were transduced with lentiviruses using polybrene (EMD Millipore, Billerica, MA) and were then selected using puromycin.

2.3. Reporter plasmids, transient transfections, and luciferase assays

The reporter plasmids used for analysis of miR122 function were constructed as described previously [12]. Plasmid transfection was performed using FuGene6 Transfection Reagent (Boehringer Mannheim, Mannheim, Germany) according to the manufacturer's instructions. pGL4-TK, a control plasmid containing *Renilla reniformis* (sea pansy) luciferase under the control of the herpes simplex virus thymidine kinase promoter (Promega, Madison, WI), was used to determine transfection efficiency. Relative luciferase values were calculated by normalizing firefly luciferase activity values to sea pansy luciferase activity values to account for changes in transfection efficiency. Luciferase activity was measured using a Dual Luciferase Reporter Assay System (Promega) with a Lumat LB9507 luminometer (EG&G Berthold, Bad Wildbad, Germany).

2.4. Northern blotting of miRNAs

Northern blotting of miRNAs was performed as described previously [23]. Briefly, total RNA was extracted using TRIzol Reagent (Invitrogen, Carlsbad, CA). Ten micrograms of RNA was resolved in denaturing 15% polyacrylamide gels containing 7 M urea in 1× TBE and then transferred to a Hybond N+ membrane (GE Healthcare, Milwaukee, WI) in 0.25× TBE. Membranes were UV-cross-linked and prehybridized in hybridization buffer. Hybridization was performed overnight at 42 °C in ULTRAhyb-Oligo Buffer (Ambion, Austin, TX) containing a biotinylated probe specific for miR122 (tgg agt gtg aca atg gtg ttt g), antisense miR122 (caa aca cca ttg tca cac tcc a), or U6 (cac gaa ttt gcg tgt cat cct t), which had previously been heated at 95 °C for 2 min. Membranes were washed at 42 °C in 2× SSC containing 0.1% SDS, and the bound probe was visualized using a BrightStar BioDetect Kit (Ambion). A pre-stained RNA size marker for small RNA (BioDynamics Laboratory, Tokyo, Japan) was used to estimate band sizes. Blots were stripped by boiling in a solution containing 0.1% SDS and 5 mM EDTA for 10 min prior to rehybridization.

2.5. Western blot analysis and antibodies

Western blotting was performed as described previously [12]. Anti-SREBP was purchased from Santa Cruz Biotechnology. Anti-β-actin was acquired from Sigma–Aldrich (St. Louis, MO). An anti-HA antibody was obtained from Roche Applied Science (Penzberg, Germany). Other antibodies were purchased from Cell Signaling Technology (Danvers, MA).

2.6. Immunohistochemistry

Tissue arrays containing liver tissues (LV1504) were purchased from US Biomax (Rockville, MD). Immunohistochemistry was performed as described previously [23]. Briefly, after deparaffinization of the slides, endogenous peroxidase activity was blocked with 3% hydrogen peroxide buffer. Antigen retrieval was achieved by incubating the slides at 89 °C in 10 mM sodium citrate buffer (pH 6.0) for 30 min. To minimize nonspecific background staining, slides were blocked in 5% normal goat serum (Dako, Glostrup, Denmark). Tissues were labeled overnight at 4 °C with primary antibodies raised against SOCS3 or SREBP1. Slides were then incubated with an anti-mouse horseradish peroxidase-conjugated secondary antibody (Nichirei Bioscience, Tokyo, Japan) for 1 h. Bound antibody was visualized by incubation in 3,3′-diaminobenzidine (Nichirei Bioscience) for 5 min. The slides were counterstained with hematoxylin, dehydrated with ethanol, and mounted using Clarion mounting medium (Biomeda, Foster City, CA).

2.7. In situ hybridization to assess miR122

Locked nucleic acid (LNA)-scramble (negative control), LNA-anti-U6 (positive control), and LNA-anti-miR122 probes were obtained from EXIQON (Vedbæk, Denmark). The expression of miR122 in liver tissues was examined by *in situ* hybridization as described previously [12]. Briefly, after deparaffinization, tissue sections were treated with 10 μg/ml proteinase K for 5 min at 37 °C, refixed with 4% paraformaldehyde, and acetylated with 0.25% anhydrous acetic acid in 0.1 M Tris–HCl buffer (pH 8.0). Following prehybridization for 30 min at 48 °C, hybridization was performed overnight with each LNA probe (20 nM) in hybridization buffer (5× SSC buffer, 50% formamide, 500 μg/ml tRNA, 50 μg/ml Cot-1 DNA). After the completion of hybridization, the sections were washed with 0.1× SSC buffer for 10 min at 52 °C three times and blocked with DIG blocking buffer (Roche Diagnostics, Basel, Switzerland) for 30 min. Sections were then probed with anti-DIG (1:500; Roche Diagnostics) for 1 h at room temperature. Detection was performed by incubation in NBT/BCIP buffer (Promega) overnight. Nuclei were stained with Nuclear Fast Red (Sigma–Aldrich).

2.8. Histological scoring

Tissue staining was scored as described previously [23]. Briefly, staining intensity was semiquantitatively categorized into the

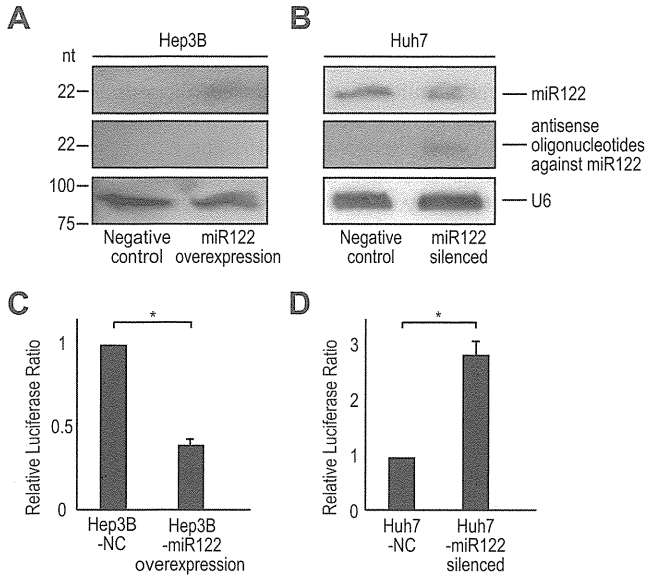

Fig. 1. Establishing of miR122-overexpressing and miR122-silenced cell lines. A, B, Northern blotting against miR122 and miR122 antisense oligonucleotides in Hep3B cells (A) and Huh7 cells (B). U6 levels were used as a loading control. Representative images from three independent experiments are shown. C, D, Luciferase expression from the reporter construct containing two tandem miR122 responsive elements in its 3'UTR, which are targeted by miR122, were examined. The suppressive effects of stably miR122 precursor-overexpressing Hep3B cells (C) and silencing effects on endogenous miR122 function in stably miR122 antisense-expressing Huh7 cells (D) are shown. Test values were normalized to those obtained from the cells transduced with a miRNA precursor-non-expressing negative control, which were set to 1 (nc). Data represent the mean ± standard deviations (SD) of three independent experiments.

following four categories by two independent investigators: –, no staining; +, weak staining; ++, moderate staining; and +++, intense staining. The color scale reflects staining intensity from green (no staining) to pink (intense staining).

2.9. Statistical analysis

Statistically significant differences between groups were determined using Student's *t*-test. *P*-values less than 0.05 were considered statistically significant.

3. Results

3.1. Establishment of miR122-overexpressing and -silenced cell lines

To determine the function of miR122, we modulated miR122 expression levels and function in liver cell lines by overexpressing an miR122 precursor construct or antisense sequences, respectively, against miR122, as previously reported [10,12]. Because Hep3B cells have relatively low miR122 expression and Huh7 cells have relatively high miR122 expression [13], we constructed miR122-overexpressing Hep3B cells and miR122-silenced Huh7 cells to examine the effects of modulating miR122. Overexpression of the miR122 precursor construct in Hep3B cells was confirmed by Northern blotting against miR122 sequences (Fig. 1A). Expression of the antisense construct against miR122 in Huh7 cells in Northern blotting appeared to be lower when using a probe to detect antisense miR122 (Fig. 1B). In these cells, miR122 levels were also lower, although miR122 was highly expressed in control Huh7 cells (Fig. 1B), suggesting that introduction of the antisense construct against miR122 may result not only in sequestration of endogenous miR122 by binding but also degradation of endogenous miR122 after formation of double-stranded RNA composed of sense and antisense miR122.

Next, we confirmed the changes in miR122 function using a luciferase reporter targeted by miR122. As predicted, in miR122-overexpressing Hep3B cells, luciferase activity decreased by more than half due to the ectopic miR122 expression (Fig. 1C). In contrast, in miR122-silenced Huh7 cells, luciferase activity increased about three times compared to control cells (Fig. 1D). These results suggest that modulation of miR122 by overexpressing exogenous constructs targeting miR122 was efficient.

3.2. SOCS3 and SREBP1 expression is decreased by miR122 silencing

Because we previously reported that miR122 silencing increased methylation in the promoter region of the SOCS3 gene and decreased its expression [10], we confirmed the expression levels of SOCS3 in miR122-overexpressing Hep3B cells and miR122-silenced Huh7 cells. Consistent with previous reports [10], SOCS3 expression increased and was downregulated in miR122-overexpressing Hep3B cells and miR122-silenced Huh7 cells, respectively (Fig. 2A and B). SOCS3 is a potent inhibitor of STAT3 activation [14]. Thus, we examined the phosphorylation status of STAT3. While total STAT3 expression levels remained unchanged, STAT3 phosphorylation decreased in miR122-overexpressing Hep3B cells and was higher in miR122-silenced Huh7 cells (Fig. 2A and B), suggesting that miR122 overexpression results in decreased STAT3 activation and that miR122 silencing has the opposite effect. Because a previous report revealed that STAT3 inhibits the promoter activity of SREBP1, a key regulator of fatty acid synthesis in the liver, we next examined the

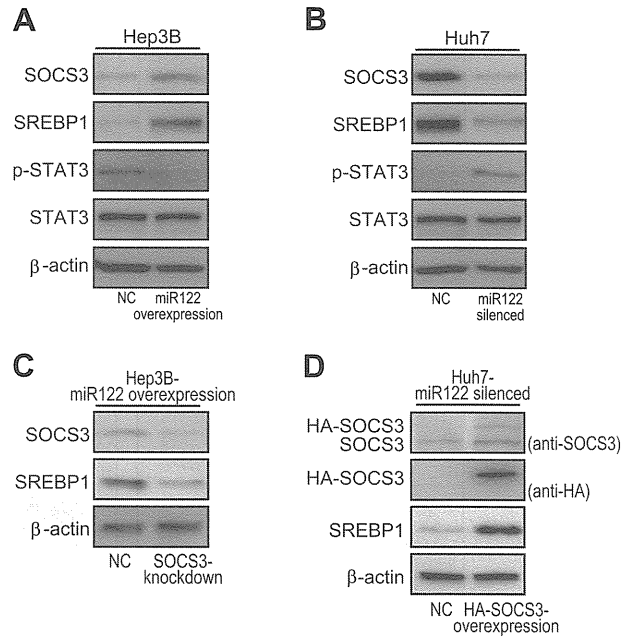

Fig. 2. SREBP1 expression is regulated by SOCS3. (A and B) SOCS3, SREBP1, and STAT3 protein expression levels and phosphorylation levels of STAT3 were determined by western blotting. Representative results from three independent experiments using Hep3B cells (A) and miR122-silenced Huh7 cells (B) are shown. (C) The effects of SOCS3 knockdown on SREBP expression in miR122 overexpressing Hep3B cell were stably transduced with SOCS3 shRNA. Representative results from three independent experiments are shown. (D) The effects of SOCS3 overexpression on SREBP expression in miR122-silenced Huh7 cells. Indicated protein expression levels were determined after miR122-silenced Huh7 cells were stably transduced with HA-SOCS3 expressing lentiviruses. HA-SOCS3 was visualized using anti-SOCS3 (the upper panel) and anti-HA (the second panel). Representative results from three independent experiments are shown.

expression levels of SREBP1 in miR122-modulated cells. The expression of SREBP1 was found to increase in miR122-over-expressing Hep3B cells and decrease in miR122-silenced Huh7 cells (Fig. 2A and B).

To confirm the role of OSCS3 in SREBP1 expression, we determined the effects of knockdown of SOCS3 expression in miR122-overexpresing Hep3B cells and enforced the expression of SOCS3 in miR122-silenced Huh7 cells (Fig. 2C and D). Knockdown of SOCS3 in miR122-overexpressing Hep3B cells reduced SREBP1 expression and enforced the expression of SOCS3 in miR122-silenced Huh7 cells increased SREBP1 expression (Fig. 2C and D). These results suggest that miR122 upregulates SOCS3 expression, resulting in the inhibition of STAT3 activation and subsequent upregulation of SREBP1 expression, and that inhibition of miR122 has the opposite effect.

3.3. Correlation of mIR122, SOCS3, and SREBP1 expression levels in human liver tissues

To confirm the above results in human clinical liver tissues, we examined 50 human liver tissues for the expression levels of miR122, SOCS3, and SREBP1 by *in situ* hybridization and immunohistochemistry (Fig. 3A and B). The expression levels of miR122 varied in liver tissues under various conditions (Fig. 3). When the expression levels of miR122 were reduced, the expression levels of SOCS3 and SREBP1 also decreased in more than 70% of cases (Fig. 3C). As previously reported [11,15], the expression levels of miR122 tended to decrease in liver cirrhosis, and SOCS3 and SREBP1 levels typically also decreased under such pathological conditions (Fig. 3C and Supplementary Table 1). These results may explain, at least in part, the decreased fatty acid and cholesterol synthesis observed clinically in the cirrhotic liver.

4. Discussion

In this study, we demonstrated that silencing miR122 function in liver cells resulted in decreased expression of SOCS3, and subsequently, decreased the expression of SREBP1. Because SREBP1 plays a key role in regulating fatty acid and cholesterol synthesis, reduced expression of miR122, which is frequently observed clinically in various chronic liver diseases [11,15], may be a cause of the decreased fatty acid and cholesterol synthesis in such pathological

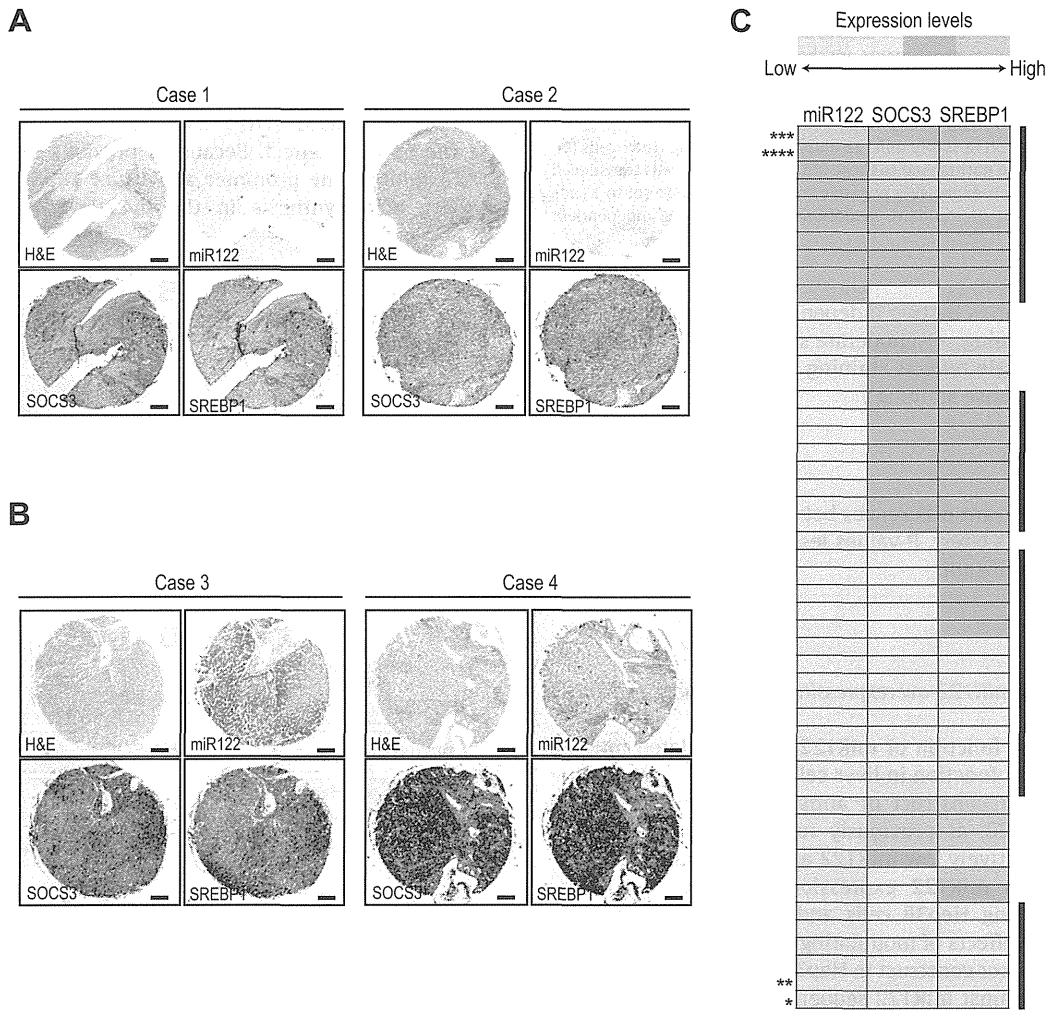

Fig. 3. Correlation of miR122, SOCS3, and SREBP expression levels in human liver tissues. (A and B), Representative liver tissues from four cases with correlated low (A) and high (B) expression levels of miR122, SOCS3, and SREBP. MiR122 was visualized by *in situ* hybridization (blue) and nuclei were stained with Nuclear Red (pink). SOCS3 and SREBP1 were stained by immunohistochemistry (brown). Bars, 500 μm. Hematoxylin and eosin (H&E)-stained tissues from each case are also shown as references. (C) Summarized expression levels of miR122, SOCS3, and SREBP1 in liver tissues from 50 cases. The color reflects the expression level of each parameter examined. Green denotes the lowest expression level and pink the highest, as the color scale bar at the top indicates. In 37 cases (indicated by black bars to the right), the differences between the expression scores of the three parameters are within one point on the color scale. *, Case 1 (A); **, Case 2 (A); ***, Case 3 (B); ****, Case 4 (B). (For interpretation of the references to color in this figure legend, the reader is referred to the web version of this article.)

states. In addition, silencing miR122 function decreases cholesterol and fatty acid levels [2–7]. While miR122 does not directly target known fatty acid-related molecules based on sequence similarities, the results of this study may explain the molecular mechanism linking miR122 silencing to decreased fatty acid and cholesterol levels.

We previously reported that silencing miR122 leads to decreased SOCS3 expression levels and increased SOCS3 promoter methylation in a Dnmt1-independent manner [10]. Such correlations in human clinical tissues were confirmed in most cases in this study. However, some cases did not show such a correlation, perhaps because while SOCS3 expression is mainly regulated by methylation of its promoter [16,17], such modifications are probably not mediated solely by miR122. Nonetheless, the decrease in SOCS3 expression that frequently accompanies decreased miR122 expression in chronic liver pathological states suggests that the SOCS3 expression in hepatocytes is largely regulated by miR122 expression or function.

The expression of SREBP1 is negatively regulated by activated STAT3, which inhibits SREBP1 promoter activities [9]. Decreased SREBP1 expression caused by increased STAT3 activity, which was itself due to decreased SOCS3 expression, was observed in miR122-silenced Huh7 cells and in liver tissues with decreased miR122 expression. Because miR122 expression levels tend to decrease as the pathological status of the liver progresses from chronic hepatitis to liver cirrhosis [11,15], observing a decreased synthesis of fatty acid and cholesterol in progressed chronic liver diseases such as liver cirrhosis may be reasonable.

One complex liver pathological situation from this point of view is obese subjects with fatty liver and insulin resistance. In these subjects, persistently elevated cytokine levels may have downregulated STAT3-mediated signaling by increasing SOCS3 protein levels in the liver [18]. Increased SOCS3 protein levels may in turn increase fatty acid synthesis by upregulating SREBP1 expression, presumably through suppression of STAT3 activation [18]. Overproduction of fatty acids and lipotoxicity result in further insulin resistance [19]. However, as these pathological conditions persist, liver cirrhosis gradually becomes apparent and fatty acid synthesis decreases. At this stage, miR122 expression in the liver becomes low [11]. Thus, in these cases, the effects of decreased miR122 expression may become apparent for the first time at the later stages of disease progression, which may be one of the reasons why not all cases showed an exact correlation between miR122 expression and SREBP levels in clinical samples.

Recently, miravirsen, an anti-miR122 oligonucleotide, was successfully applied as a novel therapeutic against HCV [7]. Although the main purpose of applying antisense miR122 *in vivo* is at present to inhibit HCV replication, decreased fatty acid and cholesterol levels were also reported [7]. In several *in vivo* experiments, antisense miR122 reduced serum lipid levels [3–5]. In addition, mice with a miR122 gene deletion in the liver showed reduced fatty acid and cholesterol levels [2,20], despite SREBP1 not being a direct target of miR122. The molecular pathway reported here may explain the reduced lipid levels observed in miR122 inhibition or gene deletion. Moreover, from these results, inhibiting miR122 may be a promising approach to controlling serum lipid levels, although the long-term inhibition of miR122 must be confirmed to be safe with no unfavorable consequences because miRNAs have pleiotropic effects [21,22].

Author contributions

C.S. and M.O. planned the research and wrote the paper. C.S., T.K., M.O., M.O., T.Y., and A.Y. performed the majority of the experiments. H.Y. supported several experiments. K.K. supervised the entire project.

Acknowledgments

This work was supported by Grants-in-Aid from the Ministry of Education, Culture, Sports, Science and Technology, Japan (#25293076 and #24390183) (to M.O. and K.K.), by Health Sciences Research Grants of The Ministry of Health, Labour and Welfare of Japan (to K.K.), and a Grant from the Japanese Society of Gastroenterology (to M.O.).

Appendix A. Supplementary data

Supplementary data associated with this article can be found, in the online version, at http://dx.doi.org/10.1016/j.bbrc.2013.07.064.

References

[1] P. Landgraf, M. Rusu, R. Sheridan, A. Sewer, N. Iovino, A. Aravin, S. Pfeffer, A. Rice, A. Kamphorst, M. Landthaler, C. Lin, N. Socci, L. Hermida, V. Fulci, S. Chiaretti, R. Foà, J. Schliwka, U. Fuchs, A. Novosel, R. Müller, B. Schermer, U. Bissels, J. Inman, Q. Phan, M. Chien, D. Weir, R. Choksi, G. De Vita, D. Frezzetti, H. Trompeter, V. Hornung, G. Teng, G. Hartmann, M. Palkovits, R. Di Lauro, P. Wernet, G. Macino, C. Rogler, J. Nagle, J. Ju, F. Papavasiliou, T. Benzing, P. Lichter, W. Tam, M. Brownstein, A. Bosio, A. Borkhardt, J. Russo, C. Sander, M. Zavolan, T. Tuschl, A mammalian microRNA expression atlas based on small RNA library sequencing, Cell 129 (2007) 1401–1414.

[2] S.H. Hsu, B. Wang, J. Kota, J. Yu, S. Costinean, H. Kutay, L. Yu, S. Bai, K. La Perle, R.R. Chivukula, H. Mao, M. Wei, K.R. Clark, J.R. Mendell, M.A. Caligiuri, S.T. Jacob, J.T. Mendell, K. Ghoshal, Essential metabolic, anti-inflammatory, and anti-tumorigenic functions of miR-122 in liver, J. Clin. Invest. 122 (2012) 2871–2883.

[3] R.E. Lanford, E.S. Hildebrandt-Eriksen, A. Petri, R. Persson, M. Lindow, M.E. Munk, S. Kauppinen, H. Ørum, Therapeutic silencing of microRNA-122 in primates with chronic hepatitis C virus infection, Science 327 (2010) 198–201.

[4] J. Elmén, M. Lindow, S. Schütz, M. Lawrence, A. Petri, S. Obad, M. Lindholm, M. Hedtjärn, H.F. Hansen, U. Berger, S. Gullans, P. Kearney, P. Sarnow, E.M. Straarup, S. Kauppinen, LNA-mediated microRNA silencing in non-human primates, Nature 452 (2008) 896–899.

[5] C. Esau, S. Davis, S.F. Murray, X.X. Yu, S.K. Pandey, M. Pear, L. Watts, S.L. Booten, M. Graham, R. McKay, A. Subramaniam, S. Propp, B.A. Lollo, S. Freier, C.F. Bennett, S. Bhanot, B.P. Monia, MiR-122 regulation of lipid metabolism revealed by *in vivo* antisense targeting, Cell Metab. 3 (2006) 87–98.

[6] J. Krützfeldt, N. Rajewsky, R. Braich, K. Rajeev, T. Tuschl, M. Manoharan, M. Stoffel, Silencing of microRNAs *in vivo* with 'antagomirs', Nature 438 (2005) 685–689.

[7] H.L. Janssen, H.W. Reesink, E.J. Lawitz, S. Zeuzem, M. Rodriguez-Torres, K. Patel, A.J. van der Meer, A.K. Patick, A. Chen, Y. Zhou, R. Persson, B.D. King, S. Kauppinen, A.A. Levin, M.R. Hodges, Treatment of HCV Infection by targeting MicroRNA, N. Engl. J. Med. 368 (2013) 1685–1694.

[8] J.D. Horton, Sterol regulatory element-binding proteins: transcriptional activators of lipid synthesis, Biochem. Soc. Trans. 30 (2002) 1091–1095.

[9] K. Ueki, T. Kondo, Y.H. Tseng, C.R. Kahn, Central role of suppressors of cytokine signaling proteins in hepatic steatosis, insulin resistance, and the metabolic syndrome in the mouse, Proc Natl Acad Sci U S A 101 (2004) 10422–10427.

[10] T. Yoshikawa, A. Takata, M. Otsuka, T. Kishikawa, K. Kojima, H. Yoshida, K. Koike, Silencing of microRNA-122 enhances interferon-[agr] signaling in the liver through regulating SOCS3 promoter methylation, Sci. Rep. 2 (2012).

[11] R.T. Marquez, S. Bandyopadhyay, E.B. Wendlandt, K. Keck, B.A. Hoffer, M.S. Icardi, R.N. Christensen, W.N. Schmidt, A.P. McCaffrey, Correlation between microRNA expression levels and clinical parameters associated with chronic hepatitis C viral infection in humans, Lab Invest. 90 (2010) 1727–1736.

[12] K. Kojima, A. Takata, C. Vadnais, M. Otsuka, T. Yoshikawa, M. Akanuma, Y. Kondo, Y.J. Kang, T. Kishikawa, N. Kato, Z. Xie, W.J. Zhang, H. Yoshida, M. Omata, A. Nepveu, K. Koike, MicroRNA122 is a key regulator of α-fetoprotein expression and influences the aggressiveness of hepatocellular carcinoma, Nat. Commun. 2 (2011) 338.

[13] S. Bai, M. Nasser, B. Wang, S. Hsu, J. Datta, H. Kutay, A. Yadav, G. Nuovo, P. Kumar, K. Ghoshal, MicroRNA-122 inhibits tumorigenic properties of hepatocellular carcinoma cells and sensitizes these cells to sorafenib, J. Biol. Chem. 284 (2009) 32015–32027.

[14] A. Yoshimura, The CIS family: negative regulators of JAK-STAT signaling, Cytokine Growth Factor Rev. 9 (1998) 197–204.

[15] K. Morita, A. Taketomi, K. Shirabe, K. Umeda, H. Kayashima, M. Ninomiya, H. Uchiyama, Y. Soejima, Y. Maehara, Clinical significance and potential of hepatic microRNA-122 expression in hepatitis C, Liver Int. 31 (2011) 474–484.

[16] B. He, L. You, K. Uematsu, K. Zang, Z. Xu, A.Y. Lee, J.F. Costello, F. McCormick, D.M. Jablons, SOCS-3 is frequently silenced by hypermethylation and suppresses cell growth in human lung cancer, Proc. Natl. Acad. Sci. USA 100 (2003) 14133–14138.

[17] Y. Niwa, H. Kanda, Y. Shikauchi, A. Saiura, K. Matsubara, T. Kitagawa, J. Yamamoto, T. Kubo, H. Yoshikawa, Methylation silencing of SOCS-3 promotes

cell growth and migration by enhancing JAK/STAT and FAK signalings in human hepatocellular carcinoma, Oncogene 24 (2005) 6406–6417.
[18] H. Tilg, The role of cytokines in non-alcoholic fatty liver disease, Dig. Dis. 28 (2010) 179–185.
[19] V.T. Samuel, K.F. Petersen, G.I. Shulman, Lipid-induced insulin resistance: unravelling the mechanism, Lancet 375 (2010) 2267–2277.
[20] W.C. Tsai, S.D. Hsu, C.S. Hsu, T.C. Lai, S.J. Chen, R. Shen, Y. Huang, H.C. Chen, C.H. Lee, T.F. Tsai, M.T. Hsu, J.C. Wu, H.D. Huang, M.S. Shiao, M. Hsiao, A.P. Tsou, MicroRNA-122 plays a critical role in liver homeostasis and hepatocarcinogenesis, J. Clin. Invest. 122 (2012) 2884–2897.
[21] G. Szabo, P. Sarnow, S. Bala, MicroRNA silencing and the development of novel therapies for liver disease, J. Hepatol. 57 (2012) 462–466.
[22] S.P. Nana-Sinkam, C.M. Croce, Clinical applications for microRNAs in cancer, Clin. Pharmacol. Ther. 93 (2013) 98–104.
[23] A. Takata, M. Otsuka, T. Yoshikawa, T. Kishikawa, Y. Hikiba, S. Obi, T. Goto, Y.J. Kang, S. Maeda, H. Yoshida, M. Omata, H. Asahara, K. Koike, MicroRNA-140 acts as a liver tumor suppressor by controlling NF-κB activity by directly targeting DNA methyltransferase 1 (Dnmt1) expression, Hepatology 57 (2013) 162–170.

J Gastroenterol
DOI 10.1007/s00535-013-0826-x

ORIGINAL ARTICLE—LIVER, PANCREAS, AND BILIARY TRACT

IL28B minor allele is associated with a younger age of onset of hepatocellular carcinoma in patients with chronic hepatitis C virus infection

Masaya Sato · Naoya Kato · Ryosuke Tateishi · Ryosuke Muroyama · Norie Kowatari · Wenwen Li · Kaku Goto · Motoyuki Otsuka · Shuichiro Shiina · Haruhiko Yoshida · Masao Omata · Kazuhiko Koike

Received: 27 September 2012 / Accepted: 22 April 2013

Abstract
Background IL28B polymorphisms were shown to be associated with a response to peg-interferon-based treatment in chronic hepatitis C (CHC) and spontaneous clearance. However, little is known about how this polymorphism affects the course of CHC, including the development of hepatocellular carcinoma (HCC). We evaluated the influence of IL28B polymorphisms on hepatocarcinogenesis in CHC patients.
Methods We genotyped the rs8099917 single-nucleotide polymorphism in 351 hepatitis C-associated HCC patients without history of IFN-based treatment, and correlated the age at onset of HCC in patients with each genotype.
Results Frequencies of TT, TG, and GG genotypes were 74.3 % (261/351), 24.8 % (87/351), and 0.9 % (3/351), respectively. The mean ages at onset of HCC for TT, TG, and GG genotypes were 69.9, 67.5 and 66.8, respectively. In multivariate analysis, IL28B minor allele (TG and GG genotypes) was an independent risk factor for younger age at onset of HCC ($P = 0.02$) in males ($P < 0.001$) with higher body mass index (BMI; $P = 0.009$). The IL28B minor allele was also associated with a lower probability of having aspartate aminotransferase-to-platelet ratio index (APRI) >1.5 (minor vs. major, 46.7 vs. 58.6 %; $P = 0.01$), lower AST (69.1 vs. 77.7 IU/L, $P = 0.02$), lower ALT (67.8 vs. 80.9 IU/L, $P = 0.002$), higher platelet count (12.8 vs. 11.2 $\times 10^4/\mu$L, $P = 0.002$), and higher prothrombin time (79.3 vs. 75.4 %, $P = 0.002$).
Conclusions The IL28B minor allele was associated with lower inflammatory activity and less progressed fibrosis of the liver; however, it constituted a risk factor for younger-age onset of HCC in CHC patients.

Keywords rs8099917 · Hepatocarcinogenesis · Interferon-λ · Risk allele · Fibrosis

Abbreviations

AFP	α-Fetoprotein
APRI	Aminotransferase platelet ratio index
CHC	Chronic hepatitis C
GWAS	Genome-wide association study
HCC	Hepatocellular carcinoma
HCV	Hepatitis C virus
IL28B	Interleukin 28B
PCR	Polymerase chain reaction
peg-IFN	peg-Interferon
RIG- I	Retinoic acid-inducible gene-I
SNP	Single-nucleotide polymorphism
SVR	Sustained viral response
TLR3	Toll-like receptor 3

Introduction

Hepatitis C virus (HCV) infection is one of the major causes of chronic hepatitis, liver cirrhosis, and hepatocellular carcinoma (HCC) [1]. Currently, patients with chronic

M. Sato · R. Tateishi · M. Otsuka · S. Shiina · H. Yoshida · K. Koike
Department of Gastroenterology, Graduate School of Medicine, The University of Tokyo, Tokyo, Japan

N. Kato (✉) · R. Muroyama · N. Kowatari · W. Li · K. Goto
Unit of Disease Control Genome Medicine, Institute of Medical Science, The University of Tokyo, 4-6-1 Shirokanedai, Minato-ku, Tokyo 108-8639, Japan
e-mail: kato-2im@ims.u-tokyo.ac.jp

M. Omata
Yamanashi Prefectural Hospital Organization, Kofu, Japan

Published online: 22 May 2013

hepatitis C (CHC) are treated with a combination of peg-interferon (peg-IFN) and ribavirin [2, 3]. Recently, HCV nonstructural 3/4A serine protease inhibitors combined with PEG-IFN and RBV were reported to achieve higher sustained viral response (SVR) rates in genotype 1 patients compared to conventional PEG-IFN/RBV. These triple therapies are considered to be the next standard of care for patients with CHC virus infection [4, 5].

Genetic variations near the interleukin 28B (IL28B) gene, encoding the type III IFN-λ3, were shown to be strongly associated with the response to peg-IFN and ribavirin treatment in patients with CHC [6–8] and also spontaneous clearance of HCV [9]. Host immune cells produce IFN and other cytokines in response to viral infection. In response to HCV, cellular sensors detect the double-stranded RNA via the retinoic acid-inducible gene-I (RIG-I) and toll like receptor 3 (TLR3) and activate a pathway to produce antiviral cytokines, including alpha and beta IFNs that trigger an antiviral response to eradicate the virus [10, 11].

Genetic polymorphisms of genes involved in innate immunities are likely to influence the strength and nature of this defense system [12]. Besides its antiviral properties, IFN-λ exhibits antitumor activity; in fact, several experimental studies in cell lines and in animal models demonstrated that the activation of type III IFN induces apoptosis [13] and antitumor activities [14–16]. Thus, this genetic factor is thought to influence the natural course of HCV infection, including the development of HCC. However, little is known about the influence of IL28B polymorphisms on hepatocarcinogenesis in patients with CHC.

In the present study, we examined the association between the rs8099917 single-nucleotide polymorphism (SNP) at the IL28B locus with the age at onset of HCC and other clinical findings in patients with CHC who had no history of receiving IFN-based treatment.

Materials and methods

Patients

The patients analyzed in the present study were derived from an HCV study cohort of the University of Tokyo Hospital. In this cohort, we enrolled the patients who visited the liver clinic at our institute between August 1997 and April 2009, and agreed to provide blood samples for human genome studies along with written informed consent according with the Declaration of Helsinki. All patients underwent laboratory blood tests at the time of enrollment in our cohort. The result of the blood tests were recorded with the information on alcohol consumption and BMI of each patient. The patients who were positive for hepatitis B surface antigen and had a history of biliary disease were excluded. All subjects in our cohort were Japanese, and this research project was approved by the ethics committees of the University of Tokyo (No. 400).

From this cohort, we examined the patients who had developed new-onset HCC and received initial therapy in our institute by January 31, 2010, and with available sample for genotyping. We excluded the patients with a history of receiving IFN-based treatment. Finally, 351 patients were enrolled for this study, and the association between the age at onset of HCC and the IL28B genotype was analyzed. Patient follow-up and Diagnosis of HCC was performed as previously described [17, 18].

IL28B genotyping

Human genomic DNA was extracted from the whole blood of each patient. Genotyping for the IL28B rs8099917 T/G polymorphism was performed by polymerase chain reaction (PCR) using the TaqMan predesigned SNP Genotyping Assay (Applied Biosystems, Foster City, CA) as recommended by the manufacturer. Allele-specific primers were labeled with fluorescent dye (FAM or HEX) and used in the PCR reaction. Aliquots of the PCR products were genotyped using an allele-specific probe of the SNP on a real-time PCR thermocycler (MX3000P, Stratagene, La Jolla, CA). Samples were subjected to 50 cycles of denaturation for 15 s at 92 °C, annealing of primers for 30 s at 60 °C, and elongation for 30 s at 60 °C.

Study endpoint

We analyzed the relationship between the age at onset of HCC (the primary endpoint of this study) and host factors, including the IL28B genotypes, sex, BMI, alcoholic consumption, and HCV genotype. We also examined the relationship between IL28B genotypes and the clinical findings at the time of enrollment in our cohort (the secondary endpoint), such as the biochemical markers and presence of liver fibrosis. Liver biopsies were only available in a small number of patients (48); liver fibrosis was assessed using the aspartate aminotransferase platelet ratio index (APRI), and an APRI of >1.5 was classified as bridging fibrosis or cirrhosis (F stage 3–4) [19].

Statistical analysis

Continuous variables were presented as the mean ± standard deviation (SD) while categorical variables were expressed as frequencies (%). Categorical data were analyzed using the Chi square test, and stepwise logistic regression analyses were used to adjust the influence of IL28B genotype by other covariates such as sex, BMI (<25

or not), and alcoholic consumption (<50 g/day or not). For continuous data, the univariate associations were evaluated using the Student's t test or nonparametric Wilcoxon rank-sum test as appropriate. Since the age at onset of HCC (the primary endpoint of this study) satisfied the assumption of normal distribution (Kolmogorov–Smirnov test, $P > 0.05$), we used stepwise regression analysis to adjust the influence of IL28B genotype by sex, BMI (<25 or not), and alcoholic consumption (<50 g/day or not). All statistical analyses were two-sided, and the threshold of the reported P values for significance was accepted as <0.05. All statistical analyses were performed using R 2.13.1 software (http://www.r-project.org).

Results

Patient characteristics

Patient characteristics are shown in Table 1. Frequencies of the rs8099917 TT, TG, and GG genotype were 74.3 % (261/351), 24.8 % (87/351), and 0.9 % (3/351), respectively. The SNP genotype distribution was in Hardy–Weinberg equilibrium (P value was not significant). We defined the IL28 major genotype as homozygous for the major sequence (TT) and the IL28B minor genotype as homozygous (GG) or heterozygous (TG) for the minor sequence. The mean age at onset of the HCC patients was 69.3 years, and approximately 60 % were male. The mean age at the time of enrollment was 67.2 years and the follow-up period was 27.9 months in average.

Table 1 Clinical characteristics and genotype distributions in the study cohort ($n = 351$)

Parameter	Values
Mean age at onset of HCC, in years	69.26 ± 8.07
Mean age at the time of enrollment, in years	67.16 ± 8.32
Male sex	200 (57.0 %)
BMI >25	70 (20.0 %)
Alcohol consumption (>50 g/day)	75 (21.4 %)
IL28B genotype	
TT	261 (74.3 %)
TG	87 (24.8 %)
GG	3 (0.9 %)
T allele frequency	0.87
HCV genotype	
Genotype 1	240 (68.4 %)
Genotype 2	91 (25.9 %)
Not tested	20 (5.7 %)

Continuous variables were represented as the mean ± standard deviation (SD) and categorical variables were as number and frequencies (%)

Primary endpoint

Table 2 shows the age at onset of patients with HCC and the associations among IL28B genotypes, sex, BMI, alcohol consumption, and HCV genotype. The mean age at onset in patients with HCC for the IL28B major and minor genotypes were 69.88 ± 7.97 and 67.48 ± 8.17, respectively, and significantly higher in patients with the IL28B major genotype than in those with the minor genotype ($P = 0.02$). In multivariate analysis, the age at onset of HCC was significantly younger in patients with the IL28B minor genotype ($P = 0.02$, Fig. 1), independently of male sex ($P < 0.001$) and higher BMI ($P = 0.009$). The characters of HCC, such as sizes (2.56 vs. 2.40 cm, $P = 0.41$) or the numbers (1.94 vs. 2.23, $P = 0.54$) at diagnosis were not significantly different between IL28B major and minor genotypes. We also analyzed the interval between blood transfusion and the onset of HCC in 161 patients who have histories of blood transfusion which had been the major cause of HCV infection in Japan [20]. The mean interval between blood transfusion and the onset of HCC for the IL28B major and minor genotypes were 39.09 ± 9.99 and 38.86 ± 9.27 years, respectively ($P = 0.9$; data not shown).

Secondary endpoint

Table 3 shows the clinical findings and associations between the IL28B genotypes at the time of enrollment in our cohort. The IL28B major genotype was significantly associated with a higher probability of having an APRI >1.5 (58.62 vs. 46.67 %, $P = 0.01$; Fig. 2), a lower platelet count (11.15 vs. 12.80 × 10^4/μL, $P = 0.002$), a higher AST level (77.69 vs. 69.12 IU/L, $P = 0.02$), a higher ALT level (80.92 vs. 67.79 IU/L, $P = 0.002$), and a lower prothrombin time (75.40 vs. 79.27 %, $P = 0.002$) compared to the IL28B minor genotype after adjustment for sex, BMI, alcoholic consumption, and the age at enrollment of our cohort. A lower γ-GTP level was significantly associated with the IL28B major genotype in univariate analysis, and alcoholic consumption, sex, and age were stronger factors associated with the γ-GTP level. Thus, after adjustment for these factors, the IL28B genotype was not extracted as a significant factor associated with the γ-GTP level. Histological assessments of liver fibrosis were performed in 248 patients at the time of initial therapy. The prevalence of histologically proved liver cirrhosis (F4) was 65.6 % (118/180) in patients with major genotype and 51.5 % (35/68) in those with minor genotype. The prevalence of liver cirrhosis was significantly higher in patients with major genotype after adjustment for sex, BMI, alcoholic consumption, and the age at the time of initial therapy for HCC ($P = 0.045$, data not shown).

Table 2 Factors associated with the age at onset of HCC

Variable	Mean	Standard deviation (SD)	*P* value	
			Univariate	Multivariate[a]
IL28B genotype			0.02	0.02
Major (TT)	69.88	7.97		
Minor (TG/GG)	67.48	8.17		
Sex			<0.001	<0.001
Male	67.94	8.48		
Female	71.02	7.16		
BMI			0.01	0.009
>25	66.87	9.11		
≤25	69.86	7.70		
Alcohol consumption			0.11	–
>50 (g/day)	67.78	9.37		
≤50 (g/day)	69.67	7.65		
HCV genotype			0.29	–
Genotype 1	69.65	7.59		
Genotype 2	68.22	8.79		

[a] Stepwise regression analysis for the age at onset of HCC (the dependent variable) using IL28B genotype, sex, BMI, alcohol consumption, and HCV genotype as independent variables

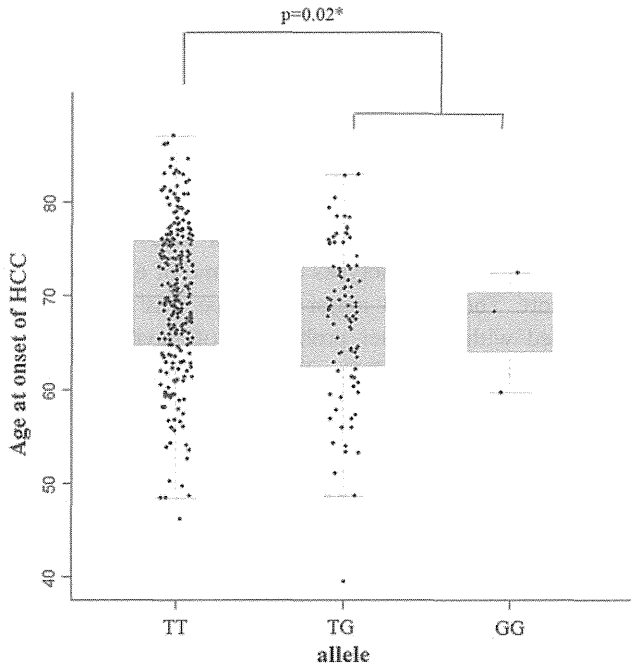

Fig. 1 *Box and whisker and dot plot* distributions of the age at onset of HCC in each genotype. The mean age at onset of HCC for the IL28B major and minor genotypes were 69.88 ± 7.97 and 67.48 ± 8.17, respectively, and was significantly higher in patients with the IL28B major genotype than in those with the minor genotype ($P = 0.02$). *P values after adjustment for sex, BMI, and alcoholic consumption

Discussion

In the present study, we evaluated the association between the IL28B polymorphism and the age at onset of HCC in patients with CHC. The IL28B minor genotype was significantly associated with younger age at onset of HCC with well known risk factors for the development of HCC such as male gender and higher BMI [21] without prior IFN-based treatment. Our previous study analyzing a susceptibility locus for HCV-induced HCC using a genome-wide association study (GWAS) could not detect the significant association between IL28B genotypes and the development of HCC in a cross-sectional distribution analysis between patients with and without HCC in more than 3,000 samples [22]. Also, IL28B alleles were not identified as a susceptibility locus for HCV-induced HCC in another GWAS study [23]. The cross-sectional distribution analyses may have underestimated the susceptibility to HCC because it could not take into consideration the future development of HCC and the duration after the past onset of HCC. Moreover, although GWAS would provide an effective and unbiased approach for revealing risk alleles for genetically complex non-Mendelian disorders, the risk of multiple comparisons made in a GWAS have resulted in reports of false positive results (Type 1 errors), and if the correction is overly conservative or the power is inadequate, false negative results (Type 2 errors) [24–26]. The relation between IL28B polymorphism and the susceptibility to HCC is still controversial. A previous study from Japan reported that the rs8099917 TT genotype was associated with a lower incidence of HCC even in non-responders to IFN based treatment [27] that was in agreement with the present study. Another study from Italy evaluating the association between genome frequency and the presence of cirrhosis due to hepatitis C, hepatitis B, alcohol use, and other factors also showed a higher prevalence of the IL28B minor allele in patients with HCC

Table 3 Associations between the IL28B genotype and clinical findings at the time of enrollment in our cohort

Variable	Mean/proportion (standard deviation; SD)		*P* values	
	Major (TT)	Minor (TG/GG)	*P* value	Adjusted *P* value[¶]
APRI >1.5[a]	58.62 % (52.38–64.66)	46.67 % (36.07–57.69)	0.07	0.01[‖]
Platelet count ($\times 10^4/\mu L$)	11.15 (5.00)	12.80 (5.43)	0.01	0.002**
AST (IU/L)	77.69 (45.14)	69.12 (38.16)	0.12	0.02**
ALT (IU/L)	80.92 (60.45)	67.79 (41.78)	0.17	0.002**
T.B (mg/dL)	0.90 (0.40)	0.83 (0.39)	0.02	–
Alb (g/dL)	3.69 (0.46)	3.71 (0.46)	0.9	–
ALP (IU/L)[b]	236.4 (81.75)	216.4 (58.96)	0.08	0.11**
γGTP (IU/L)[c]	76.83 (65.34)	87.23 (42.92)	0.005	–
PT (%)[d]	75.40 (13.36)	79.27 (13.13)	0.02	0.002**

[¶] Adjusted for sex, BMI, alcoholic consumption, and the age at enrollment (independent variables). The dependent variables of each *P* values are the items in the leftmost fields of corresponding rows (the proportion of having APRI >1.5, platelet count, AST, ALT and so on)

[‖] *P* value by stepwise logistic regression analysis

** *P* value by stepwise regression analysis

[a] Odds ratio (95 % CI) for major allele was 1.88 (1.13–3.11), and 95 % confidence interval (CI) of each proportion is parenthesized for this outcome

[b] Missing in 115 patients

[c] Missing in 112 patients

[d] Missing in 4 patients

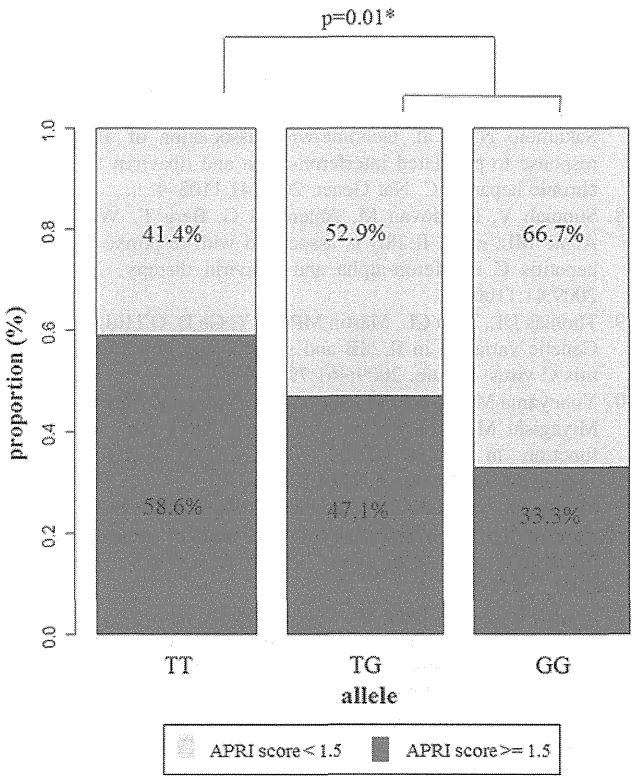

Fig. 2 *Bar plot* the proportion of having an AST-to-platelet ratio (APRI) score >1.5 in each allele. **P* values after adjustment for sex, BMI, alcoholic consumption, and the age at enrollment

compared to those without HCC [28]. However, other studies showed no relation between IL28B polymorphism and the susceptibility to HCC [29–32]. Some studies have reported the HCV genotype 1 as a risk factor associated with HCC in patients who had CHC [33–35]; however, we could not find a significant association between the HCV genotype and hepatocarcinogenesis in the present study. Our data showed no relationship between the duration of HCV infection in the patients with a history of blood transfusion. The mean age of blood transfusion was not significantly different between patients with major and minor genotypes (28.99 in major genotype vs. 27.60 in minor genotype, $P = 0.18$). Moreover, older age at HCV infection was reported to be associated with more rapid disease progression [36]. Thus, the difference in the duration of HCV infection may have little effect on the result of the present study. The IL28B genotype may have a critical role in the onset of HCC. Moreover, only about 45 % of all patients in the present study have the history of blood transfusion; hence, further analysis with larger samples may be indicated.

Previous studies evaluating patients with chronic HCV infection showed severer histological inflammatory activity and fibrosis, as well as higher ALT levels and APRI scores in patients homozygous for the IL28B major alleles [29, 32, 37, 38]. Similarly, in the present study, the IL28B

major genotype was significantly associated with a higher probability of having an APRI >1.5 and a higher ALT level; and the prevalence of histologically proved liver cirrhosis (F4) was significantly higher in patients with major genotype at the age at the time of initial therapy for HCC. Given the association between the IL28B major allele and the severe inflammatory activity or progressed fibrosis, the IL28B allele is thought to be associated with the susceptibility to HCC via a mechanism that is independent of controlling an activity of HCV infection.

Recent experimental studies have suggested that IFN-λ has an antitumor activity. In esophageal cancer cell lines expressing IFN-λ receptor complexes, IFN-λ1 suppressed growth via the induction of the G1 phase arrest or apoptosis [39]. An antitumor activity of IFN-λ was also shown in the B16 melanoma, BNL hepatoma, Colon 26, and neuroendocrine BON1 tumor cells [40–43]. One probable explanation for the paradoxical result of the present study is that the more aggressive inflammatory activity of patients with IL28B major genotype may reflect a stronger immune response to the virus, which may also have anti-tumor effects. However, the innate immune responses and antitumor activity via IFN-λ, as well as the mechanism underlying the association of the IL28B genotype, have not been elucidated. Further studies are needed to determine the functional role of the IL28B gene in relation to the course of chronic HCV infection, including hepatocarcinogenesis.

Because of the retrospective design, this study is limited by the absence of some important clinical details such as information about the histological findings of fibrosis and inflammation. Although the APRI is a useful index for the prediction of fibrosis, the limitation of this score has been reported in previous studies [44, 45]. Prospectively designed studies are needed to confirm our findings. However, observing chronic HCV-infected patients without antiviral treatment would be nearly impossible in the future. In this regard, the present study may have important implications.

In conclusion, the IL28B minor genotype was associated with a younger age of onset of HCC in patients with CHC, and this association was completely independent of the response to IFN-based treatment. Hepatocarcinogenesis appeared to be suppressed in patients who had CHC with the IL28B major genotype, despite higher inflammatory activity and progressed fibrosis of liver. The current findings may provide a clinically important information in the follow-up or HCC screening of cirrhotic patients.

Acknowledgments This study was supported by the Global COE Program, "Center of Education and Research for Advanced Genome-Based Medicine: For personalized medicine and the control of worldwide infectious diseases"; the Ministry of Education, Culture, Sports, Science and Technology, Japan; by grants from the Leading Project of the Ministry of Education, Culture, Sports, Science and Technology, Japan; and by Health and Labor Sciences Research Grants for Research on Hepatitis from the Ministry of Health, Labor and Welfare, Japan.

Conflict of interest None of the authors have any conflicts of interest.

References

1. Barrera JM, Bruguera M, Ercilla MG, Gil C, Celis R, Gil MP, et al. Persistent hepatitis C viremia after acute self-limiting posttransfusion hepatitis C. Hepatology. 1995;21:639–44.
2. Hadziyannis SJ, Sette H Jr, Morgan TR, Balan V, Diago M, Marcellin P, et al. Peginterferon-alpha2a and ribavirin combination therapy in chronic hepatitis C: a randomized study of treatment duration and ribavirin dose. Ann Intern Med. 2004;140:346–55.
3. Manns MP, McHutchison JG, Gordon SC, Rustgi VK, Shiffman M, Reindollar R, et al. Peginterferon alfa-2b plus ribavirin compared with interferon alfa-2b plus ribavirin for initial treatment of chronic hepatitis C: a randomised trial. Lancet. 2001;358:958–65.
4. McHutchison JG, Everson GT, Gordon SC, Jacobson IM, Sulkowski M, Kauffman R, et al. Telaprevir with peginterferon and ribavirin for chronic HCV genotype 1 infection. N Engl J Med. 2009;360:1827–38.
5. Poordad F, McCone J Jr, Bacon BR, Bruno S, Manns MP, Sulkowski MS, et al. Boceprevir for untreated chronic HCV genotype 1 infection. N Engl J Med. 2011;364:1195–206.
6. Ge D, Fellay J, Thompson AJ, Simon JS, Shianna KV, Urban TJ, et al. Genetic variation in IL28B predicts hepatitis C treatment-induced viral clearance. Nature. 2009;461:399–401.
7. Tanaka Y, Nishida N, Sugiyama M, Kurosaki M, Matsuura K, Sakamoto N, et al. Genome-wide association of IL28B with response to pegylated interferon-alpha and ribavirin therapy for chronic hepatitis C. Nat Genet. 2009;41:1105–9.
8. Suppiah V, Moldovan M, Ahlenstiel G, Berg T, Weltman M, Abate ML, et al. IL28B is associated with response to chronic hepatitis C interferon-alpha and ribavirin therapy. Nat Genet. 2009;41:1100–4.
9. Thomas DL, Thio CL, Martin MP, Qi Y, Ge D, O'Huigin C, et al. Genetic variation in IL28B and spontaneous clearance of hepatitis C virus. Nature. 2009;461:798–801.
10. Yoneyama M, Kikuchi M, Natsukawa T, Shinobu N, Imaizumi T, Miyagishi M, et al. The RNA helicase RIG-I has an essential function in double-stranded RNA-induced innate antiviral responses. Nat Immunol. 2004;5:730–7.
11. Moriyama M, Kato N, Otsuka M, Shao RX, Taniguchi H, Kawabe T, et al. Interferon-beta is activated by hepatitis C virus NS5B and inhibited by NS4A, NS4B, and NS5A. Hepatol Int. 2007;1:302–10.
12. Li CZ, Kato N, Chang JH, Muroyama R, Shao RX, Dharel N, et al. Polymorphism of OAS-1 determines liver fibrosis progression in hepatitis C by reduced ability to inhibit viral replication. Liver Int. 2009;29:1413–21.
13. Li W, Lewis-Antes A, Huang J, Balan M, Kotenko SV. Regulation of apoptosis by type III interferons. Cell Prolif. 2008;41:960–79.
14. Numasaki M, Tagawa M, Iwata F, Suzuki T, Nakamura A, Okada M, et al. IL-28 elicits antitumor responses against murine fibrosarcoma. J Immunol. 2007;178:5086–98.
15. Li M, Liu X, Zhou Y, Su SB. Interferon-lambdas: the modulators of antivirus, antitumor, and immune responses. J Leukoc Biol. 2009;86:23–32.